Prepared for submission to JINST

European Conference on Plasma Diagnostics 2021
7 June - 11 June 2021
Zoom

# Development of the Q-band ECE Imaging system in the Large Helical Device

**Y. Goto,**[a,1] **T. Tokuzawa**[a] **D. Kuwahara**[b] **K. Ichinose**[c] **H. Tsuchiya,** [d,2] **M. Nishiura**[a] **T. Shimizu**[a] **S. Kubo**[b] **I. Yamada**[a]

[a] *National Institute for Fusion Science, National Institute of Natural Sciences, Toki, Japan*
[b] *College of Engineering, Chubu University, Kasugai, Japan*
[c] *Department of Applied Energy, Nagoya University, Nagoya, Japan*
[d] *System Technology Development Center, Kawasaki Heavy Industries, Ltd., Tokyo, Japan*

*E-mail:* goto.yuki@nifs.ac.jp

Abstract: In this study, we developed the Electron Cyclotron Emission Imaging (ECEI) system with the Q-band in the Large Helical Device (LHD). ECEI measurement makes it possible to obtain the spatiotemporal structure of magnetohydrodynamics (MHD) instabilities in the high-$\beta$ plasma. Although there were several difficulties for realizing the multi-channelization, such as local oscillator (LO) optics and an expensive high-power LO source, we have solved these problems by developing a Local Integrated Antenna array (LIA) which has an internal LO supply, using a frequency doubler integrated circuit on each channel, instead of a conventional Horn-antenna Mixer Array (HMA) with common LOs. In addition, we have made some improvements to enhance the quality of the measurement signal. First, we developed and introduced notch filters that prevent the strong Electron Cyclotron Resonance Heating (ECRH) stray signal from being mixed into the measurement circuit. Second, the position of the doubler built in the printed circuit board was reconsidered to prevent the mixing of higher harmonic components into the mixer. Also, we have adopted the Logarithmic detector (LOG detector) to deal with the wide dynamic range of the plasma fluctuation. After these improvements, for the first time, we could successfully obtain the initial results of the two-dimensional temperature distribution and its fluctuation distribution in the LHD.

Keywords: Microwave Antennas; Microwave radiometers; Detector design and construction technologies and materials; Plasma diagnostics - interferometry, spectroscopy and imaging

[1] Corresponding author.
[2] Former National Institute for Fusion Science, National Institute of Natural Sciences.

## Contents



## 1 Introduction

Electron Cyclotron Emission (ECE) measurement is one of the key tools for obtaining an electron temperature profile because the ECE's frequency and intensity are proportional to the magnetic field strength and electron temperature, respectively [1, 2]. Therefore, by arranging the ECE measurement system in an array, it is possible to observe the two-dimensional temperature distribution with high temporal resolution in plasma. This is called ECE Imaging (ECEI) measurement. ECEI can be a powerful tool for measuring the spatiotemporal structure of the temperature and its fluctuations caused by magnetohydrodynamics (MHD) or other instabilities in high-$\beta$ plasma. For this reason, ECEI measurement has been carried out intensively in recent years [3, 4].

In the Large Helical Device (LHD), ECEI measurement has been performed on a high-$\beta$ plasma with a central magnetic field strength of 1 T. As shown in figure 1(a), the frequency band was selected at the Q-Band (35 to 42 GHz) for focusing on measuring the second harmonic $X$-mode on the edge of LHD plasma. This means that the measurement region is the rational surface with $m/n = 1/1$ where the rotational transform $\iota$ becomes $\iota = 1$. Here, $m$ and $n$ are the poloidal and toroidal mode numbers. As in the ECEI system, it is possible to separate the ECE signal into eight frequency bands (channels) per antenna by a filter bank. In this research, we finally manufactured a radiometer array with eight antennas, resulting in 64 channels in total. In the 22nd LHD experimental campaign, we have successfully obtained two-dimensional temperature fluctuations in the LHD for the first time. This was enabled by a breakthrough regarding millimeter-wave components. By replacing the method of local oscillator (LO) signal supply from the conventional Horn antenna Mixer Array (HMA) by the Local Oscillator Integrated Antenna Array (LIA), we could solve issues described in references [5, 6]. In addition, we have made some improvements to enhance the quality of the measurement signal. First, we developed and introduced notch filters that prevent the strong Electron Cyclotron Resonance Heating (ECRH) stray signal from being mixed into the measurement circuit. Second, the position of the multiplier built in the printed circuit board was reconsidered to prevent the mixing of higher harmonic components into the mixer. Also, we have adopted the Logarithmic detector (LOG detector) to deal with the wide dynamic range of the plasma fluctuation. Thus, the system could be simplified and the performance could be improved.

This paper is composed of four sections. In section 2, our ECEI system is briefly described. In

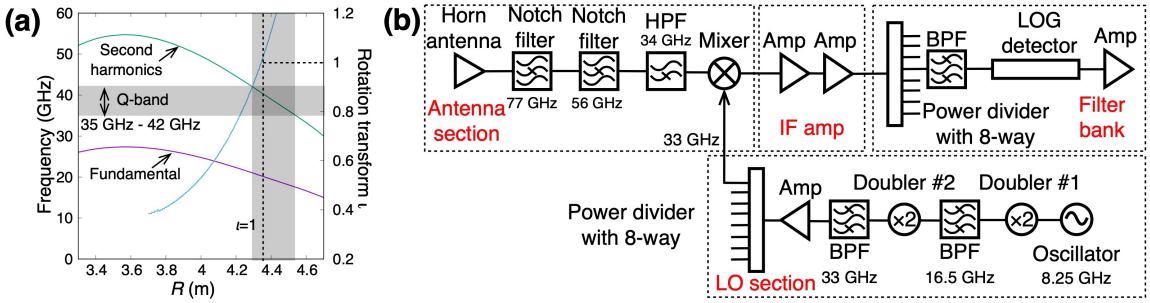


**Figure 1**. (a) Measurement region in major radius $R$ corresponding to the Q-band with 35 GHz to 42 GHz. (b) Heterodyne detection system with LIA for ECEI measurement. This system has eight antennas, and the ECE signal can be divided by eight frequency bands (channels) per antenna, resulting in 64 channels in total.

section 3, the initial results of the two-dimensional temperature fluctuations measurement in LHD are discussed. A summary of this paper is provided in section 4.

## 2 Development of the Measurement System

Figure 1(b) shows the ECEI system we developed for the LHD experiment. ECE signals are transmitted from LHD plasma to this system by five reflecting mirrors [7]. In this system, the Intermediate Frequency (IF) is divided into eight channels. The bandwidth at -3 dB is ±0.4 GHz and the corresponding spatial resolution is less than 35 mm in the radial direction. Also, the bandwidth at -10 dB is ±0.5 GHz. The frequency band from 35 to 42 GHz (eight channels) means the center frequency. Therefore, for example, when we focus on "35 GHz" with bandwidth -10 dB, 35 ± 0.5 GHz is measured. As we mentioned, the following three important breakthroughs and improvements made it possible to measure the two-dimensional temperature fluctuations in the LHD.

First, we have developed two types of notch filters, which reject only specific frequencies. It supports 56 GHz and 77 GHz. In the 56 GHz notch filter, the attenuation is achieved at more than 50 dB, and the bandwidth at -3 dB is 1.1 GHz. Also, in the 77 GHz notch filter, the attenuation is achieved at more than 55 dB, and the bandwidth at -3 dB is 1.6 GHz [8]. In the LHD, 56 GHz and 77 GHz gyrotrons are used for heating the plasma and the nominal powers of 56 GHz and 77 GHz gyrotrons have ~ 500 kW and ~ 1 MW, respectively. Since these frequencies are adjacent to the Q-band, they affect the ECE measurement. By developing and introducing these notch filters in this system, it was possible to eliminate the interference of measurement by ECRH. Second, the doubler #2 originally built into the antenna section was replaced with the Local Oscillator(LO) section. Conventionally, frequencies such as 8.25, 16.5, and 66 GHz, and so on were generated by the doubler #2, and these signals also were mixing in the mixer. These made it difficult to distinguish from the original IF signal. Therefore, the doubler #2, which was originally in the antenna section, was isolated to the LO section so that only 33 GHz could enter the mixer by BPF (Band Pass Filter). Also, we have successfully confirmed that the LO signals do not transmit to the IF section through the mixer. Because 8.25 GHz and 16.5 GHz signals generated at the LO section are significantly attenuated by the BPFs after doubler #1 and doubler #2, respectively. Moreover, the 16.5 GHz signal is out of the detection band of the IF amplifier and LOG detector, even if the signal transmits to the IF section through the mixer. Finally, we introduced a LOG detector to deal with the wide

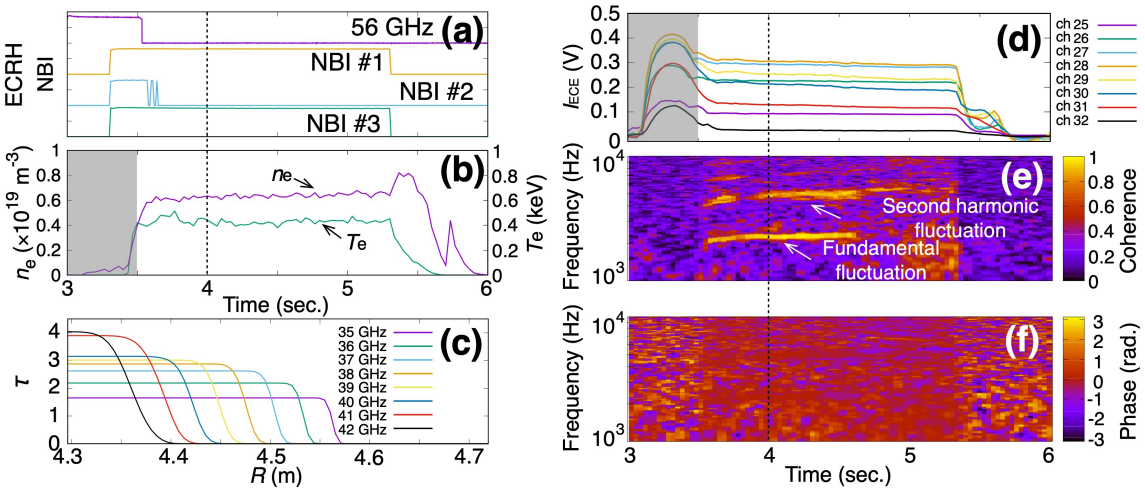


**Figure 2**. (a) ECRH with 56 GHz injection timing and NBIs injection timing; (b) Electron density and electron temperature at the measurement point corresponding to ch 27; (c) Optical thickness at the measurement region with $z = 0$ and $t = 4$ sec; (d) Raw ECE signals from ch 25 (35 GHz) to ch 32 (42 GHz) shown in figure 3(b); (e) and (f) Cross correlation spectra and the phases between center channel (ch 29) and ch 25.

dynamic range of the plasma fluctuations, which has a -50 dBm minimum limit of detection and a typical 45 dB dynamic range. In the conventional system using linear detector, the signal inversion was observed due to the saturation of the IF amplifier. Although this can be solved by adjusting the attenuator, it is not realistic because it is difficult to predict the signal level and access to the device hall for maintenance during the experimental period. However, by introducing the LOG detector for improving the dynamic range, we have successfully obtained an ECE signal. Considering the performance of each section, the minimum limit of detection, as the antenna input, has -90 dBm.

## 3 Initial Results of the ECEI Measurement

In the 22nd LHD experimental campaign, high-$\beta$ plasma was investigated under the condition of the magnetic field strength 1 T and the magnetic axis 3.6 m on the shot number #163518. Then, we have successfully obtained two-dimensional temperature fluctuations by using the heterodyne detection system we developed for the first time.

In the experiment, as shown in figure 2(a), the plasma was initiated by 56 GHz ECRH and sustained by the neutral beam injection (NBI) after 3.5 sec. Then, the plasma has an electron density $n_e = 0.6 \times 10^{19}$ m$^{-3}$ at the measurement region and an electron temperature $T_e = 0.4$ keV at the measurement region, and is stably sustained from 3.5 sec. to 5.3 sec. as shown in figure 2(b). These plasma parameters were obtained from the Thomson scattering measurement at each time slice mapped on the flux surfaces. In addition, as shown in figure 2(c), the optical thickness $\tau$ at the measurement region with $z = 0$ and $t = 4$ sec. is greater than one in every center frequency. Thus, the line-of-sight is optically thick in this experiment. Then, we obtained the ECE signals as shown in figure 2(d). These are raw ECE signals corresponding to the measurement cross section shown in figure 3(b) from ch 25 to ch 32. As can be seen, even in the period when the ECRH is applied, the influence of the strong stray signal due to ECRH does not appear in the ECE signals, and it can

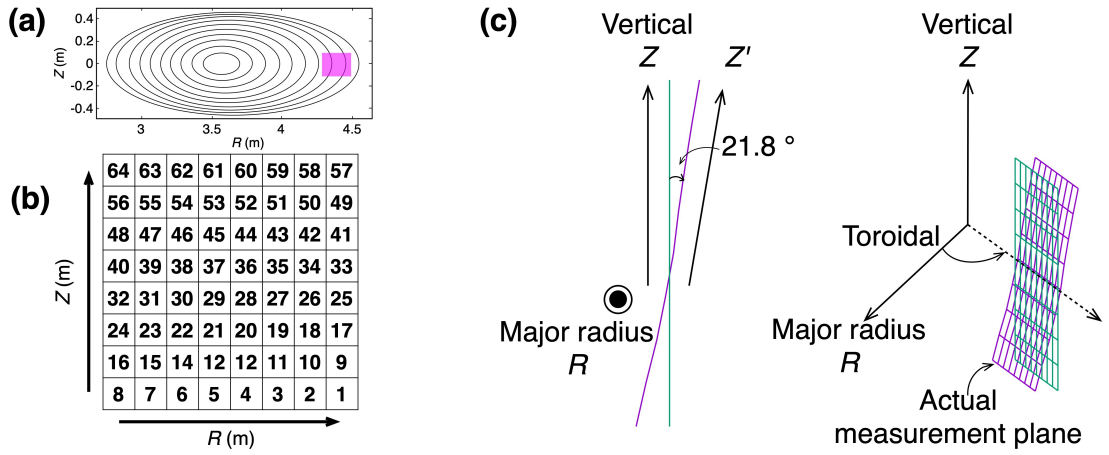


**Figure 3**. (a) Horizontally-elongated plasma cross section. The purple region is the measurement region. (b) Channel arrangement at the measurement region. (c) Actual measurement cross section.

be seen that the notch filter is working effectively. A comparison with the case where the notch filter is not introduced is described in detail in the reference [8]. Note that the ECE raw signals do not reflect the electron temperature measured by the Thomson scattering measurement from 3.1 to 3.5 sec. This is because the plasma has not produced yet in this period. Thus, the ECE signals do not correspond to $T_e$ in this period, although there is a probability that the non-thermal ECE is measured. In addition, by introducing a LOG detector, we succeeded in detecting a wide range of ECE signals. Thus, we have confirmed that these signals corresponding to the electron temperature with a sufficient S/N ratio are obtained on all channels. Figure 2(e) and (f) show the time variation of the cross correlation and the phase between center channel 29 and ch 25. As can be seen, 2 kHz and 4 KHz, and the higher harmonic spectra were detected after around 3.5 sec. It can also be seen that the phases concerning those spectra have a certain characteristic phase. Since there are no harmonics signals due to our measurement circuit, owing to the improvement as mentioned above, it is considered that the observed cross correlation spectra are due to the fluctuation of the plasma. Thus, we can obtain the time evolution of the two-dimensional structures of the ECE signal.

Before that, we would like to explain the measurement cross section in this experiment. In this experiment, attempted measurements were carried out in the region where MHD instability occurs, as shown in figure 3(a). The ECEI system can measure this area with 64 channels, as shown in figure 3(b). In figure 3(a) and (b), the vertical axis represents the vertical direction. However, note that the measurement cross section is actually tilted by 21.8 degrees, as shown in figure 3(c). Therefore the vertical axis is expressed as $z'$ instead of $z$.

In order to obtain a two-dimensional electron temperature distribution and a two-dimensional electron temperature fluctuation distribution, we carried out a calibration of the raw ECE signal from voltage to temperature by comparing the Thomson scattering measurement data which is interpolated by the VMEC (equilibrium calculation code) and the raw ECE signal data. At this time, we assume that the relationship between voltage and temperature is linear within 3.5 sec. to 5.3 sec. This assumption can be made because there is no time change of the electron temperature in the period and the ECE signals are almost constant as well, as shown in figure 2(b) and (d).

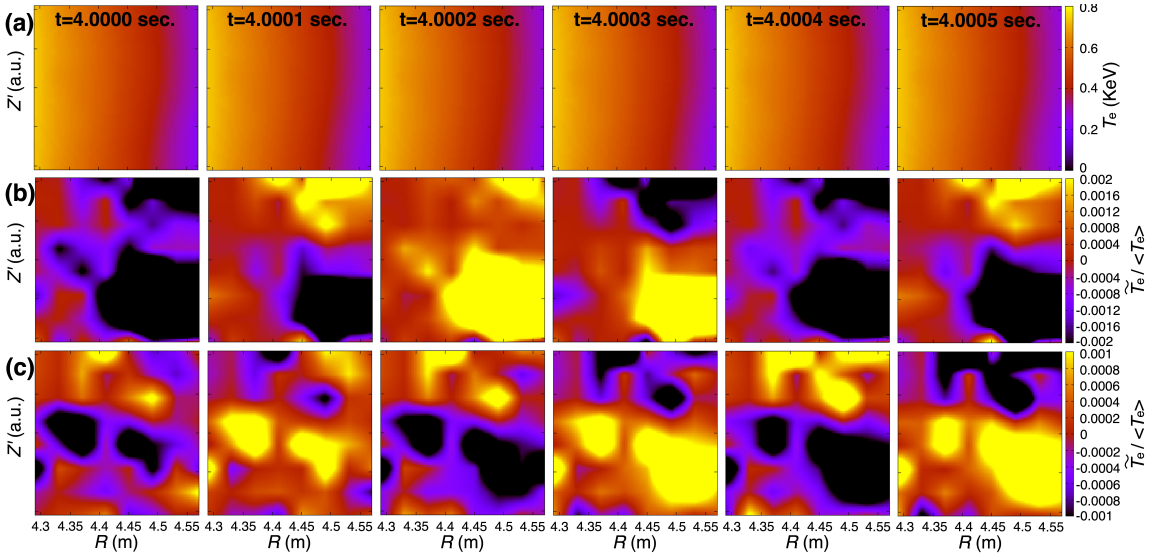


**Figure 4**. (a) Two-dimensional electron temperature distribution. (b) Two-dimensional the electron temperature fluctuation intensity distribution at the fundamental fluctuation spectra peak. (c) Two-dimensional the electron temperature fluctuation intensity distribution at the second harmonics fluctuation spectra peak.

With this calibration, we composed the two-dimensional electron temperature distribution and the two-dimensional electron temperature fluctuation distribution. Figures 4(a), (b), and (c) show the time variation of the two-dimensional electron temperature distribution, the electron temperature fluctuation distribution regarding fundamental spectral, and the electron temperature fluctuation distribution regarding second harmonics spectral. Here, $< T_e >$ represents an ensemble average of the electron temperature and $\tilde{T}_e$ represents the difference between the electron temperature and the ensemble average, that is, $\tilde{T}_e \equiv T_e - < T_e >$. In addition, these two-dimensional distributions were interpolated from 8 ch $\times$ 8 ch to 100 ch $\times$ 100 ch.

As can be seen, the electron temperature distribution does not change with time at first sight. However, it can be seen that the fluctuation distribution has periodicity. In the case of the fundamental fluctuation, its frequency is 2 kHz and its period is 0.5 msec. Focusing on the lower right region, $\tilde{T}_e / < T_e >$ initially has a negative value, but it becomes a positive value with time and returns to a negative value again after just 0.5 msec. On the other hand, in the case of the second harmonic fluctuation, its frequency is 4 kHz and its period is 0.25 msec. As with the fundamental fluctuation, $\tilde{T}_e / < T_e >$ starts at a negative value and returns to a negative value again in 0.25 msec via a positive value. Therefore, we have successfully obtained the time evolution of the two-dimensional temperature distribution and its fluctuation distribution for the first time in the LHD by realizing the multi-channelization of the ECE measurement system.

## 4 Summary

In this study, we developed the Q-band ECEI system with the LIA and could successfully obtain the initial results of the two-dimensional temperature distribution and its fluctuation distribution in the LHD for the first time. In order to obtain the two-dimensional temperature fluctuations and its

fluctuation distribution in the LHD, we have carried out three important improvements of the ECEI system. One is the development of notch filters. Thanks to this filter, we were able to reject strong ECRH stray signals from mixing the ECEI measurement system. Second, we guaranteed a pure LO signal with 33 GHz by placing a doubler #2 in the LO section. As a result, the purity of the IF signal can be ensured, and the fluctuation signal has been successfully obtained. And finally is the introduction of the LOG detector. By introducing the LOG detector for improving the dynamic range, we have successfully obtained the ECE signal. This result will contribute to understanding the cause of MHD instability and turbulence analysis.

In addition, in this study we focus on our attention on obtaining the spatial structure of the electron temperature fluctuation distribution by developing millimeter-wave components. However, in the ECEI system, it is also important to determine the spatial resolution accurately, as well as to obtain the spatial structure of the electron temperature fluctuation distribution. Although the spatial resolution in the radial direction has been considered from the performance of the filter bank, the spatial resolution in the $z$ direction has not been determined yet and it should be estimated in future. Actually, we are trying to estimate the resolution by using the ECE calculation method, using ray-tracing described in reference [2], which can calculate the beam spreading. Then we will be able to develop the ECEI system that has accurate spatial resolution as well.

## Acknowledgments

The authors would like to thank the LHD experiment group for its excellent support of this work. This work was partially supported in part by KAKENHI (Nos. 19H01880 and 21H04973), by a budgetary Grant-in-Aid from the NIFS LHD project, under the auspices of the NIFS Collaboration Research Program (ULPP051).

## References

[1] G. Bekefi, "*Radiation Processes in Plasmas*", Wiley, (1966)

[2] Y. Goto et al., *Development of the calibration method for a fast steering antenna for investigating the mode conversion window used in EBW heating in the LHD plasma*, Jpn. J. Appl. Phys. **58** (2019) 106001

[3] H. K. Park et al., *Comparison Study of 2D Images of Temperature Fluctuations during Sawtooth Oscillation with Theoretical Models*, Phys. Rev. Lett. **96** (2006) 195004

[4] Y. Zhu et al., *W-band system-on-chip electron cyclotron emission imaging system on DIII-D*, Rev. Sci. Instrum. **91** (2020) 093504

[5] D. Kuwahara et al., *Development of electron cyclotron emission imaging system on Large Helical Device*, Rev. Sci. Instrum. **81**, (2010) 10D919

[6] D. Kuwahara et al., *Development of local oscillator integrated antenna array for microwave imaging diagnostics*, JINST **10** (2015) C12031

[7] H. Tsuchiya et al., *Installation of New Electron Cyclotron Emission Imaging in LHD*, Plasma Fusion Res. **13** (2018) 3402063

[8] M. Nishiura et al., *Q-band high-performance notch filters at 56 and 77 GHz notches for versatile fusion plasma diagnostics*, Rev. Sci. Instrum. **92**, (2021) 034711